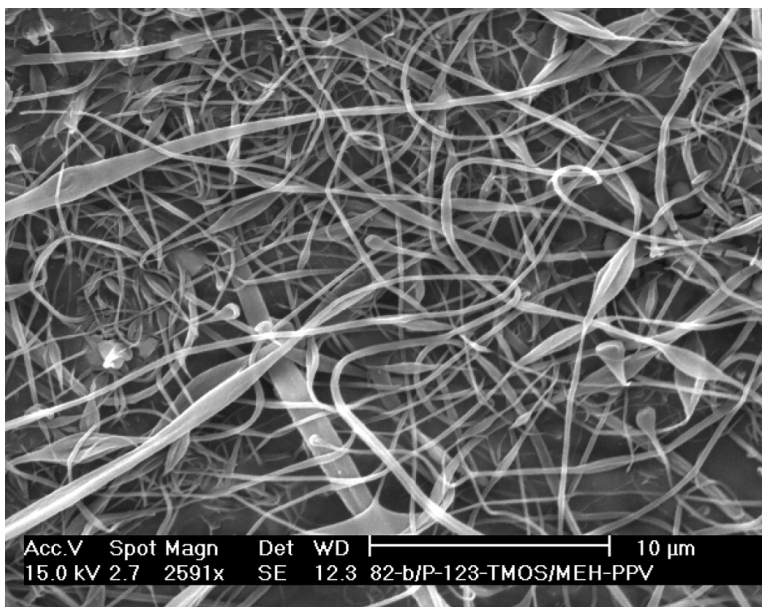


Electrospun MEH-PPV/SBA-15 Composite Nanofibers Using a Dual Syringe Method

Sudha Madhugiri, Alan Dalton, Jose Gutierrez, John P. Ferraris, and Kenneth J. Balkus

J. Am. Chem. Soc., **2003**, 125 (47), 14531-14538 • DOI: 10.1021/ja030326i • Publication Date (Web): 31 October 2003

Downloaded from <http://pubs.acs.org> on March 30, 2009



More About This Article

Additional resources and features associated with this article are available within the HTML version:

- Supporting Information
- Links to the 23 articles that cite this article, as of the time of this article download
- Access to high resolution figures
- Links to articles and content related to this article
- Copyright permission to reproduce figures and/or text from this article

[View the Full Text HTML](#)

Electrospun MEH-PPV/SBA-15 Composite Nanofibers Using a Dual Syringe Method

Sudha Madhugiri, Alan Dalton, Jose Gutierrez, John P. Ferraris, and
Kenneth J. Balkus Jr.*

*Contribution from the Department of Chemistry and The UTD NanoTech Institute,
University of Texas at Dallas, Richardson, Texas 75083-0688*

Received May 29, 2003; E-mail: balkus@utdallas.edu

Abstract: The process of electrospinning, which produces fibers in the nanometer to micron range under the influence of high voltages, has been widely studied to produce polymer and textile fibers. Mesoporous molecular sieve fibers have been produced in our lab, and this technique was extended to produce an interwoven mesh of polymer–molecular sieve composite fibers. The electroluminescent polymer MEH-PPV and molecular sieve SBA-15 were used to produce the composite fibers. An interesting aspect of these composites is that the fluorescence of MEH-PPV is blue shifted in the composites. The composites have been characterized by microscopy, vibrational spectroscopy, and fluorescence measurements.

Introduction

The optoelectronic properties of poly(paraphenylene vinylene) (PPV) polymers have generated a great deal of interest.¹ These conjugated polymers are potential materials for several applications such as light emitting diodes (LEDs) and photovoltaic devices. One interesting member of the PPV family is poly[2-methoxy-5-(2'-ethyl-hexyloxy)-1,4-phenylenevinylene] (MEH-PPV) shown in Figure 1a, which is electroluminescent and has been widely studied for its optoelectronic properties.^{2–6} However, in the solid state, these PPV derivatives seem to fail because of the aggregates and defects. The interchain interactions of the polymer, which are more prevalent in the solid state, can lead to the aggregates and lower performance. Extended conjugation lengths also lead to emissions at higher wavelengths. Therefore, the ability to control the optical properties of these polymers could lead to improvements in the performance by these polymers in the optoelectronic devices. Efforts include the introduction of side chains in the polymer, which make them more soluble and can reduce the interaction between the polymer chains.⁷ Also the introduction of nanospacers such as carbon nanotubes has been explored to limit interchain interactions.^{8–9} The present work involves the preparation of a nonwoven mesh

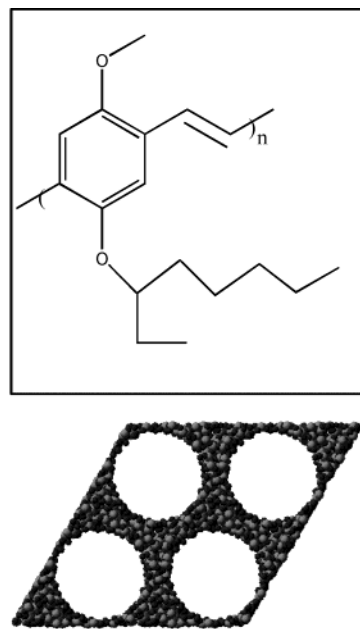


Figure 1. (a) Structure of MEH-PPV and (b) a representation for SBA-15.

of MEH-PPV and all silica mesoporous molecular sieve fibers via electrospinning.

Composites of PPV derivatives and inorganic materials have been studied from a variety of perspectives. For example, the process of energy transport in MEH-PPV has been studied by inclusion of the polymer within an oriented mesoporous silica host.^{5,10} Charge transfer in photovoltaics has also been studied by forming nanocomposites of conjugated polymers with semiconducting, porous TiO₂ and SnO₂.^{11,12} Mesoporous mo-

- (1) Moses, D.; Dogariu, A.; Heeger, A. J. *Chem. Phys. Lett.* **2000**, *316*, 356.
- (2) Kraft, A.; Grimsdale, A. C.; Holmes, A. B. *Angew. Chem., Int. Ed.* **1998**, *37*, 402.
- (3) Arango, A. C.; Carter, S. A.; Brock, P. J. *Appl. Phys. Lett.* **1999**, *74*, 1698.
- (4) Padmanabhan, G.; Ramakrishnan, S. *J. Am. Chem. Soc.* **2000**, *122*, 2244.
- (5) Schwartz, B. J.; Nguyen, T. Q.; Wu, J.; Tolbert, S. *Synth. Met.* **2001**, *116*, 35.
- (6) Long, F. H.; McBranch, D.; Hagler, T. W.; Robinson, J. M.; Swanson, B. I.; Pakbaz, K.; Schicker, S.; Heeger, A. J.; Wudl F. *Mol. Cryst. Liq. Cryst.* **1994**, *256*, 121.
- (7) Gettenger, C. L.; Heeger, A. J.; Drake, J. M.; Pine, D. J. *J. Chem. Phys.* **1994**, *101*, 1673.
- (8) Dalton, A. B.; Coleman, J. N.; in het Panhuis, M.; McCarthy, B.; Drury, A.; Blau, W. J.; Paci, B.; Nunzi, J. M.; Byrne, H. J. *J. Photochem. Photobiol., A* **2001**, *144*, 31.
- (9) Ago, H.; Shaffer, S. P. M.; Ginger, D. S.; Windle, A. H.; Friend, R. H. *Phys. Rev. B* **2000**, *61*, 2286.

- (10) Nguyen, T. Q.; Wu, J.; Tolbert, S. H.; Schwartz, B. J. *Adv. Mater.* **2001**, *13*, 609.

lecular sieves comprise an important class of inorganic materials and have been widely studied for their tunable pore size and morphology. The potential application in catalysis, separations, chemical sensors, dielectric coatings, and a wide variety of other areas drive this research. Many of these applications would benefit from a fibrous form. SBA-15 is one such class of surfactant templated mesoporous material synthesized by Stucky and co-workers which has been prepared as fibers.^{13–16} Figure 1b shows a representation of SBA-15. More recently, a hexagonal mesoporous material DAM-1 (Dallas Amorphous Materials #1) has also been shown to form in various distinct shapes.¹⁷ These molecular sieve materials have been synthesized in different forms, but the technique of electrospinning had not been applied to produce molecular sieve fibers. We have recently shown that a network of mesoporous fibers of these materials can be obtained via electrospinning.¹⁸

Electrospinning is a technique that can be used to produce high surface area nanofibers under the influence of an electrostatic field.^{19–23} Polymers such as poly(ethylene oxide), poly-L-lactide, and polyaniline have been electrospun. We have electrospun mesoporous fibers of the all silica materials SBA-15 and DAM-1¹⁸ as well as pure MEH-PPV fibers in our lab.²⁴ Molecular sieve fibers are inherently brittle, and therefore, it was hoped that electrospinning an organic polymer and the inorganic fibers together would result in composite fibers which couples the functionality of the mesoporous material with the flexibility and processibility of the polymer. To this end, we have employed a novel dual syringe electrospinning method to prepare a composite fiber network of a semiconducting, electroluminescent, polymer MEH-PPV and mesoporous SBA-15 silica. We have found that the composite fibers obtained by electrospinning MEH-PPV and SBA-15 together exhibit a blue shift in the polymer emission while maintaining the same excitation spectrum as compared to pure MEH-PPV fibers. In addition, when SBA-15 containing phenyl silane is electrospun with MEH-PPV, a further shift to blue (with an emission in green) is observed. In addition to fluorescence, the fibers were characterized by SEM, FT-IR, Raman, and XRD.

Experimental Section

MEH-PPV has been synthesized according to the published procedure with modifications.²⁵ The molecular weights of the samples used were 292 000 (Mn) with a polydispersity of 1.04 and 281 000 (Mn)

with a polydispersity of 1.58. Fibers of MEH-PPV were electrospun using 7–10 wt % solutions of the polymer in 1,2-dichloroethane (Aldrich) using the sample with a polydispersity of 1.04. The sample with a broader polydispersity (1.58) formed more of a beaded fiber. The gel for electrospinning SBA-15 fibers was prepared as follows.¹⁸ The surfactant P-123 (BASF), a poly(ethylene oxide)–poly(propylene oxide)–poly(ethylene oxide) triblock copolymer (EO₂₀PO₇₀EO₂₀), tetramethoxysilane (TMOS) (Aldrich), ethanol (Aaper Alcohol), 2 M hydrochloric acid (HCl) (EM Science), and water were combined in the molar ratio of 0.0026 P-123:0.0600 TMOS:0.2605 ethanol:0.0082 2 M HCl:0.1044 H₂O for this gel. The required amount of P-123 was dissolved in a mixture of ethanol and 2 M HCl under constant stirring at room temperature. TMOS was then added dropwise under constant stirring at room temperature to form a clear solution having a pH of ~1. Whenever an organosilane such as (phenyltrimethoxysilane (ph-TMS)) trimethylchlorosilane (TMCS) and phenyldimethylchlorosilane (PDMCS) (Gelest Inc) was used, the required amount of organosilane was substituted for the equivalent number of moles of TMOS. The synthesis gel was heated in a glass beaker uncovered at 60–70°C until the desired viscosity (~14 000 cP) was obtained. Typically, 10 mL of the solution were heated for ~50–60 min to obtain a gel for electrospinning. When heated, partial hydrolysis and condensation of silica occurs along with the slow evaporation of the solvent (ethanol/methanol) forming a clear, viscous gel. A dual syringe system was used to electrospin MEH-PPV and SBA-15 together (see Supporting Information for details).

Two syringes one containing MEH-PPV solution and the other containing SBA-15 gel were subjected to a voltage of 20 kV (Sorensen H. V. Supply model # 1020-30). A distance of 22–24 cm was maintained between the tip of the syringe and the substrate. The fibers formed were collected on an HCl treated anopore filter with a 25 mm diameter (Fisher Scientific) mounted on aluminum foil. Acid treatment was necessary for SBA-15 fibers to form, ensuring complete hydrolysis of TMOS.¹⁸

The morphology, density, and thickness of Au/Pd coated fibers were evaluated using a Philips XL30 scanning electron microscope (SEM), and the presence of Si in the composite samples was mapped using EDAX. Fluorescence spectra were recorded from the Jobin Yvon Spex fluorimeter using Datamax software. As the samples were electrospun onto opaque substrates such as aluminum, excitation and emission spectra were obtained using a sample holder placed at 45° to the UV light source and the emitted light was collected at a 90° angle. To obtain the absorption maximum for the polymer and the composite samples, the emission monochromator was set at a certain wavelength, and a range of excitation wavelengths were scanned to obtain an excitation spectrum. The emission monochromator was set at 550 nm for MEH-PPV fibers, and excitation wavelengths were scanned from 300 to 540 nm. The λ_{max} obtained from the excitation spectrum was used as an excitation wavelength for the emission spectrum.

FTIR spectra for the bulk were recorded using a Nicolet Avatar 360 spectrophotometer. Micro-FTIR spectra were recorded using a Perkin-Elmer Spectrum GX system on samples directly electrospun onto KBr pellets, and micro-Raman spectra were obtained using a Jobin Yvon Horiba system using Lab Spec software exciting the samples using a 633 nm laser.

Results and Discussion

Applying 20 kV to an MEH-PPV or an SBA-15 gel leads to the formation of a fine jet. When the particles of the jet overcome the surface tension, they form a fine jet.^{19–21} The conical shaped jet travels and eventually deposits on the target. The idea behind using two different solutions was to make an interwoven network of fibers containing a polymer and a molecular sieve material and study the optical properties of the resulting composite.

- (11) Christiaans, M. P. T.; Wienk, M. M.; Van Has, P. A.; Kroon, J. M.; Janssen, R. A. J. *Synth. Met.* **1999**, *101*, 265.
- (12) Anderson, N. A.; Hao, E.; Ai, X.; Hastings, G.; Lian, T. *Chem. Phys. Lett.* **2001**, *347*, 304.
- (13) Marlow, F.; McGehee, M. D.; Zhao, D.; Chmelka, B. F.; Stucky, G. D. *Adv. Mater.* **1999**, *11*, 632.
- (14) Yang, P.; Zhao, D.; Chmelka, B. F.; Stucky, G. D. *Chem. Mater.* **1998**, *10*, 2033.
- (15) Zhao, D.; Sun, J.; Li, Q.; Stucky, G. D. *Chem. Mater.* **2000**, *12*, 275.
- (16) Dongyuan, Z.; Jinyu, S.; Quanzhi, L.; Stucky, G. D. *Chem. Mater.* **2000**, *12*(2), 275.
- (17) Balkus, K. J., Jr.; Coutinho, D.; Lucas, J.; Washmon-Kriel, L. *Mater. Res. Soc. Symp. Proc.* **2001**, *628*, cc10.7.1.
- (18) Madhugiri, S.; Ferraris, J. P.; Balkus, K. J., Jr. *Microporous Mesoporous Mater.* **2003**, *63*, 75.
- (19) Norris, D.; Shaker, M. M.; Ko, F.; MacDiarmid, A. G. *Synth. Met.* **2000**, *114*, 109.
- (20) Reneker, D. H.; Chun, I. *Nanotechnology* **1996**, *7*, 216.
- (21) Dietzel, J. M.; Kleinmeyer, J.; Harris, D.; Beck Tan, N. C. *Polymer* **2000**, *41*, 261.
- (22) Bognitzki, M.; Czado, W.; Frese, T.; Schaper, A.; Hellwig, M.; Steinhart, M.; Greiner, A.; Wendroff, J. H. *Adv. Mater.* **2001**, *13*, 70.
- (23) Fong, H.; Chun, I.; Reneker, D. H. *Polymer* **1999**, *40*, 4585.
- (24) Madhugiri, S. Dissertation, University of Texas at Dallas, 2002.
- (25) Neef, C. J.; Ferraris, J. P. *Macromolecules* **2000**, *33*, 2311.

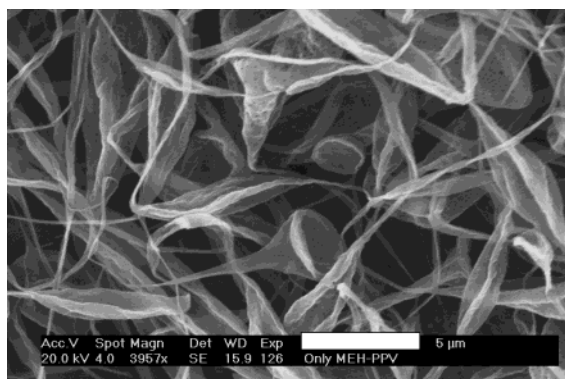


Figure 2. SEM image of MEH-PPV fibers after a 5 min deposition.

MEH-PPV was electrospun using a 7–10 wt % solution in 1,2-dichloroethane. Although MEH-PPV dissolves in solvents such as chloroform, tetrahydrofuran, benzene, 1,2-dichlorobenzene, and toluene, the boiling point of 1,2-dichloroethane (76–78 °C) was conducive for electrospinning. An SEM image of pristine MEH-PPV (pd 1.04) is shown in Figure 2. Typically the resulting fibers are approximately 200 nm in diameter with many exhibiting a leaflike structure. In some places, the leaflike structures appear like two or more fibers fused together, while, in other regions, they appear like ribbons. This morphological variation may be due to the viscosity of the polymer solution (350–400 cp at 0.07 rpm), which could not be increased due to the upper limit on polymer solubility.

SEM images of the dual electrospun deposit of MEH-PPV and SBA-15 together reveals a dense fibrous network. The average diameter of the fibers is about 700–800 nm (Figure 3a and b). However, the amount of leafy structures seen in pure MEH-PPV fibers (Figure 2) is markedly reduced in the MEH-PPV/SBA-15 composite. The fibers are also continuous and well-defined relative to those formed from the pure polymer. After a ~5 min deposition, a mesh of 2–3 μm thickness is obtained as shown in Figure 3c.

Additional proof for the presence of both of the types of fibers in the composite was obtained from inspection of the XRD patterns for the composite. An XRD pattern characteristic of SBA-15 fibers was obtained for the MEH-PPV/SBA-15 composite fibers (Figure 4a). SEM images obtained for the composite before and after calcination (for MEH-PPV removal) also show the presence of SBA-15 fibers in the composite (Figure 4b and c, respectively). The mesoporosity of the fibers is clearly evident from the XRD pattern with a *d* spacing corresponding to 90.1 Å. This closely agrees with the literature values for the silica fibers drawn from precursor solutions using P-123 as the surfactant.¹⁴ The TEM image of the obtained SBA-15 fibers is shown in Figure 5 and clearly shows a two-dimensional hexagonal pore structure. The fibers formed by electrospinning are probably partially condensed clusters of mesoporous silica. The condensation is better facilitated by deposition onto an acid-treated substrate. As the fibers were wig-l-bug treated to reduce the particle size for TEM analysis, the pore size of the fibers could not be clearly determined.

Micro-IR spectroscopy and Raman scattering were used to identify and characterize the two different types of materials present in the composite. Two completely different IR spectra were obtained for the composite fiber samples as shown in Figures 6 and 7. The spectrum labeled c was obtained from

SBA-15 fibers in the composite. Spectrum a obtained for the bulk molecular sieve and spectrum b for pure SBA-15 fibers are shown for comparison. In these spectra, the feature in the region 1100–1000 cm⁻¹ is attributed to the Si–O–Si asymmetric stretch which overlaps with the peak obtained in the same region for pure SBA-15 fibers and bulk SBA-15 (Figure 6b and c). A broad feature at 1365 cm⁻¹ can be attributed to C–C stretching and deformation belonging to the –CH₂ groups present in the P-123 which is used as a template for the formation of SBA-15 fibers. Peaks observed at 2910 and 2852 cm⁻¹ (region not shown) are attributed to asymmetrical and symmetrical C–H stretches of –CH₂ groups belonging to P-123.²⁵

The micro-IR spectrum of an MEH-PPV fiber in the composite (Figure 7c) was compared to pure MEH-PPV fibers (Figure 7b) and bulk MEH-PPV (Figure 7a). The assignments are summarized in Table 1. When the micro-IR spectrum of an MEH-PPV fiber is compared to the IR spectrum of bulk MEH-PPV (Figure 7a and b), a shift of about ≤10 cm⁻¹ to lower wavenumbers in the fiber samples is observed. In addition, the vibrational modes corresponding to C=C centered at 1600 cm⁻¹ are softened in the fibers. The combination of these two results suggests that the polymer in the fiber form is morphologically different when compared to bulk (vide infra). The broad bands in the region 3000–3500 and a broad peak at 1700 cm⁻¹ in the spectra are due to water. All the peaks listed in Table 1 correspond well with the expected range of vibrational stretches reported for MEH-PPV.^{26–30} The *cis*-vinylene C–H stretch, which normally appears in the region 650–730 cm⁻¹, could not be seen as the micro-IR spectrometer scans between 4000 and 700 cm⁻¹. However, a peak corresponding to a *cis*-vinylene stretch was absent in the IR spectrum of the bulk sample also. Therefore, it can be assumed that the sample of MEH-PPV used exists predominantly in the *trans* configuration. When the fibers of MEH-PPV were dissolved and the FTIR spectra obtained, the recovered bulk polymer was essentially the same as the starting material (data not shown). The micro-IR spectra of pure MEH-PPV fibers and the MEH-PPV in the composite samples (Figure 7b and c) are essentially the same, which suggests that spectroscopically the polymer is similar in both pure and composite fibers. The polymer and the composite samples were further characterized by Raman spectroscopy. Raman scattering has been shown to be a powerful technique to probe structure–property relationships in conjugated polymers. In particular, this technique has been extensively used to observe the C=C stretches of paraphenylene vinylene (PPV) derivatives which have been shown to produce a characteristic triplet in the 1500–1700 region.^{6,27–29} This is evident in the spectra shown in Figure 8. The strong peak at 1586 cm⁻¹ with two shoulders at 1529 and 1621 cm⁻¹ are characteristic for the PPV derivatives. The 1586 cm⁻¹ mode corresponds to the symmetric stretch of the phenyl group, and the one at 1621 cm⁻¹ corresponds to the C=C stretch of the vinylenic group. The mode at 1114 cm⁻¹ is the C–H rocking mode of the phenyl group. The mode observed

(26) Silverstein, R. M.; Webster, F. X. *Spectrometric Identification of Organic Compounds*; John Wiley and Sons: New York, 1997; Chapter 3.

(27) Tein B.; Zerbi, G.; Schenk, R.; Mullen, K. *J. Chem. Phys.* **1991**, *95*, 3191.

(28) Tein B.; Zerbi, G.; Schenk, R.; Mullen, K. *J. Chem. Phys.* **1991**, *95*, 3198.

(29) *Raman Spectroscopy Theory and Practice*; Szymanski, A. H., Ed.; Plenum Press: New York, 1967.

(30) Bradley, D. D. C.; Friend, R. H.; Lindenberger, H.; Roth, S. *Polymer* **1986**, *27*, 1709.

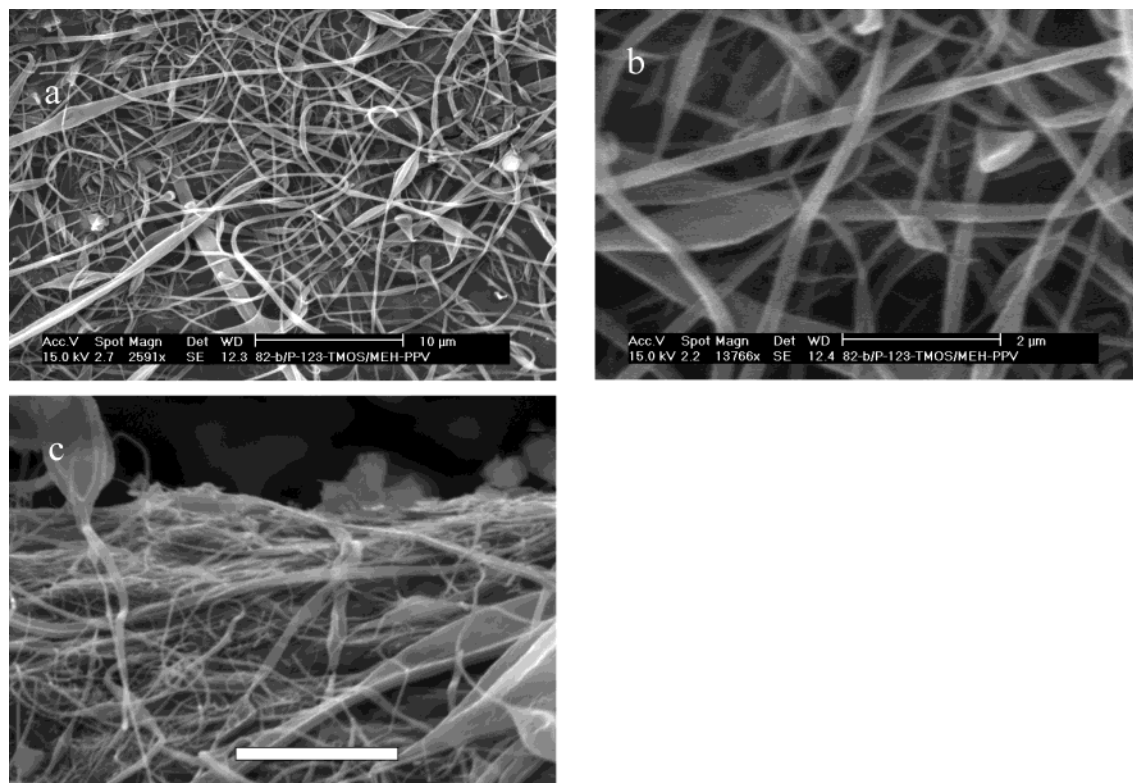


Figure 3. SEM images of (a) an electrospun MEH-PPV/SBA-15 composite fiber mesh from a 5 min deposition and (b) a composite fiber mesh (c) a composite fiber mesh image at a 40° tilt angle.

at 603 cm^{-1} is analogous to the 605 cm^{-1} band observed in benzene. When the Raman spectra of MEH-PPV fibers (spectrum b in Figure 8) and MEH-PPV/SBA-15 (spectra c and d in Figure 8) composite fibers are compared, the Raman bands in the composite samples show a downshift of about $4\text{--}5\text{ cm}^{-1}$. This mode softening has previously been associated with an extension in conjugation suggesting that in the composite samples polymer strands are forced into an extended conformation possibly induced by nanofiber formation.^{27,28} To further probe the structure–property modification in the fibers compared to the bulk, selective area microphotoluminescence spectra were taken by exciting the samples using a 404 nm source. While vibrational spectroscopy of the MEH-PPV in the form of fibers suggests higher order in the polymer chains compared to the bulk, the interesting result is that the luminescence of MEH-PPV in the electrospun composite is blue shifted relative to the bulk. The shift in the luminescence was quantified using macro- and microluminescence, and the changes in the optical properties were correlated with the vibrational spectroscopy of the samples. To further investigate the role of compositing MEH-PPV with the silica material, phenyltrimethoxysilane was introduced in the reaction mixture of SBA-15. This should enhance the interaction between the polymer and the inorganic material. As a result of this, it was observed that the emission of the composite was further blue shifted to green. A digital image of the fluorescence and the emission spectra are shown in Figures 9 and 10, respectively.

An excitation spectrum with a λ_{max} of 467 nm was obtained (see Supporting Information) for MEH-PPV fibers. Subsequently, emission spectra were obtained exciting the sample at 467 nm which produced an emission maximum of 593 nm (Figure 10a). Similar excitation and emission spectra were taken

for the MEH-PPV/SBA-15 composite fibers. The excitation spectrum obtained for the composite was the same as the excitation spectrum of the pure MEH-PPV fibers with an absorption λ_{max} of 467 nm. However, the emission spectrum showed a 27 nm blue shift in the emission with a λ_{max} of 566 nm (Figure 10b).

The similarity of the excitation (absorption) spectra of MEH-PPV and MEH-PPV/SBA-15 composite suggests that the chromophore in both sets of fibers is same. The blue shift observed in the case of composite fibers can possibly be due to two reasons. There could have been a disruption in the conjugation length or prevention of aggregation in the polymer when electrospun along with the mesoporous silica. Both of these reasons are known to cause a blue shift in the emission of fluorescent polymers. Partially conjugated MEH-PPV has been shown to emit at about 57 nm less than the fully conjugated MEH-PPV.³¹ However, in our case, vibrational spectroscopy suggests that break in conjugation might not be the case.

To better understand these phenomena, excitation spectra for MEH-PPV fibers and MEH-PPV/SBA-15 composite fibers were recorded by setting the emission at wavelengths in the red and in the blue regions of the electromagnetic spectrum. However, the excitation spectra were exactly the same in all cases for both the MEH-PPV and the composite fibers with the λ_{max} being 467 nm (Figure 3i in the Supporting Information). In a similar manner, emission spectra were recorded as the samples were excited at various wavelengths. Similar emission spectra were obtained in all the cases (Figure 3ii in the Supporting Information). This indicates that the chromophore responsible for the absorption and emission is the same in both the samples. The

(31) Wood, P.; Samuel, I. D. W.; Weseter, G. R.; Burn, P. L. *Synth. Met.* **2001**, *119*, 571.

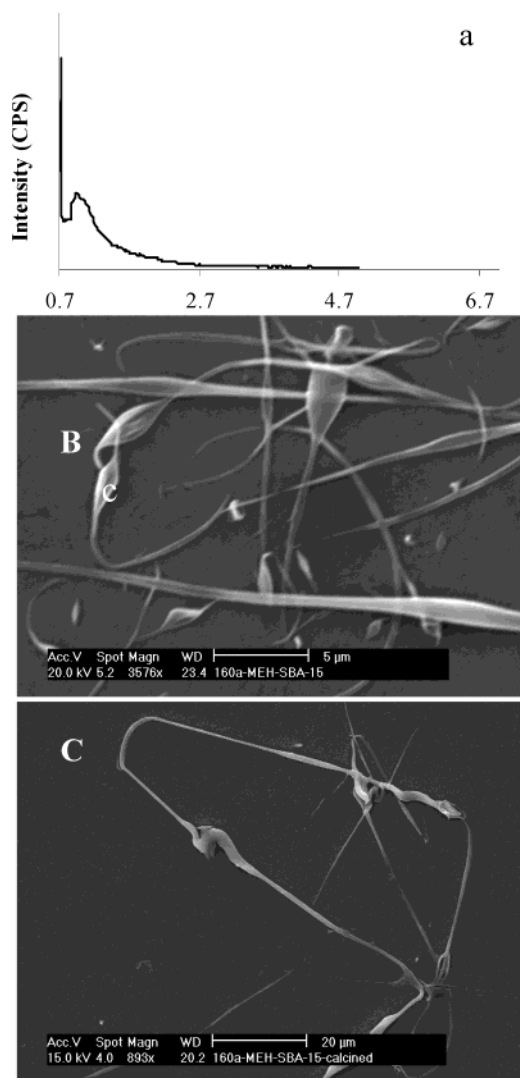


Figure 4. (A) XRD pattern for the SBA-15/MEH-PPV composite fibers, (B) SEM image of the SBA-15/MEH-PPV, and (C) after calcination.

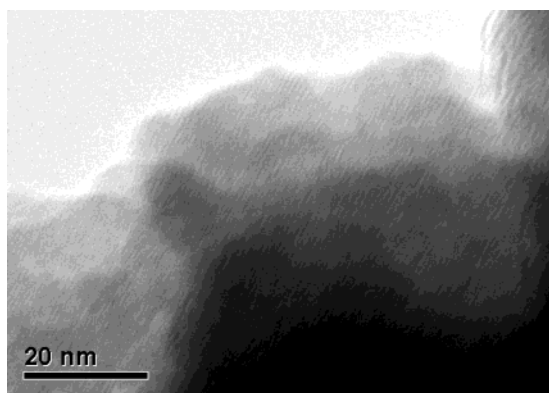


Figure 5. TEM image of SBA-15 fibers which are part of the MEH-PPV/SBA-15 composite.

vibrational spectroscopy suggests an extension in the conjugation of the polymer molecule which should have produced a red shift in the emission when compared to bulk. However, the blue shift produced in the emission suggests that there is a possible prevention of aggregation in the polymer fiber in the composite.

To further examine the reason for the change in optical properties, fluorescence data were collected for solutions of MEH-PPV in 1,2-dichloroethane and a film of MEH-PPV. The

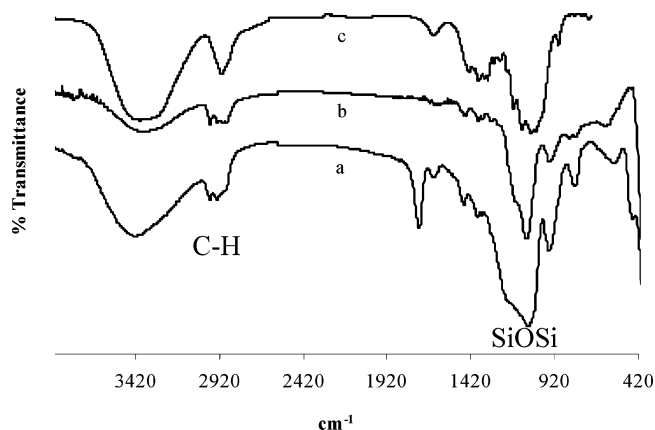


Figure 6. FTIR spectra of (a) bulk SBA-15, (b) pure SBA-15 fibers, and (c) an individual fiber from the composite.

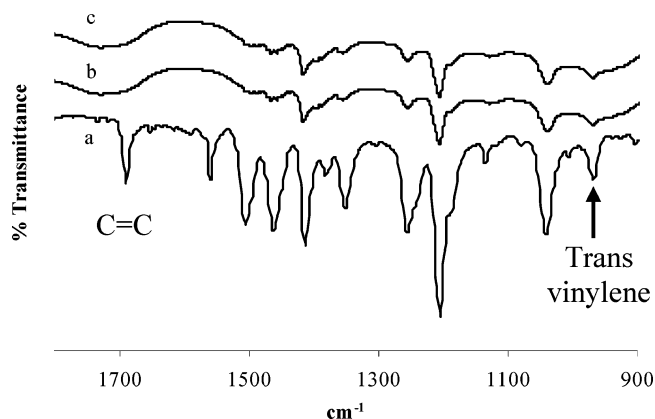


Figure 7. FTIR spectra of MEH-PPV (a) bulk and (b) pure MEH-PPV fibers and (c) an individual fiber of MEH-PPV in the composite.

Table 1. Analysis of IR Spectra of Fibers Belonging to MEH-PPV

infrared bands observed in bulk MEH-PPV (cm ⁻¹)	infrared bands observed in a fiber (cm ⁻¹)	assignment
2960	2935	asymmetric C—H stretch in —CH ₃ group
2931	2921	asymmetric C—H stretch in —CH ₂ group
2871/2873	2855/2854	symmetric C—H stretch in —CH ₂ group
1691	broad water peak	C=C stretch
1560	missing	C—C ring stretch
1508	broad peak	C—C ring stretch
1463	1455	asymmetric C—H bending in —CH ₃ group
1413	1411	ring stretch and C—H deformation mode
1353	1349	C—C stretch and C—H deformation
1255	1250	aryl—alkyl ether (C—O—C) asymmetric stretch
1205	1205	ring stretch and C—H deformation
1043	1035	aryl—alkyl ether (C—O—C) symmetric stretch
1135	1113	C—H in-plane bend
970	966	trans vinylene C—H out-of-plane bend

solution in 1,2-dichloroethane (10^{-7} M) has an emission λ_{\max} of 559 nm,²⁴ and for a spin cast film, the values of absorption and emission are 467 and 599 nm, respectively (Figure 11).²⁴

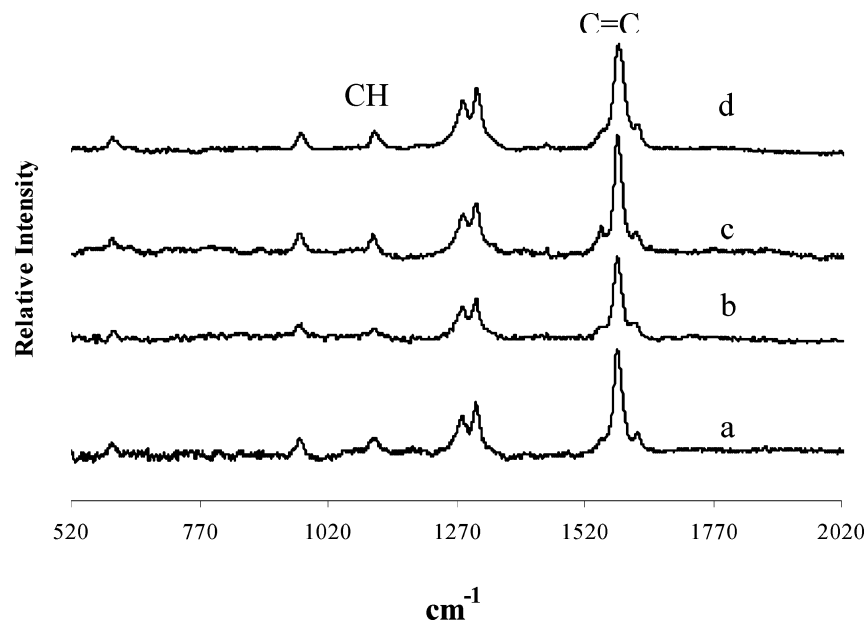


Figure 8. Raman spectra of (a) bulk MEH-PPV and (b) MEH-PPV fibers, (c) MEH-PPV/SBA-15 composite fibers, and (d) MEH-PPV/(SBA-15 with phenyltrimethoxysilane) composite fibers.

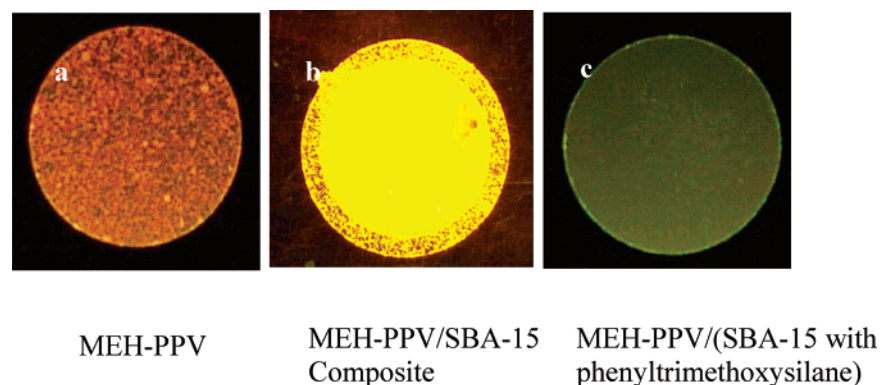


Figure 9. Digital images of emission colors of (a) MEH-PPV, (b) the MEH-PPV/SBA-15 composite, and (c) the MEH-PPV/(SBA-15 with phenyltrimethoxysilane) composite. Samples a and c were electrospun onto an HCl-treated microscope cover slip, and sample b was electrospun onto an anapore filter (20 nm).

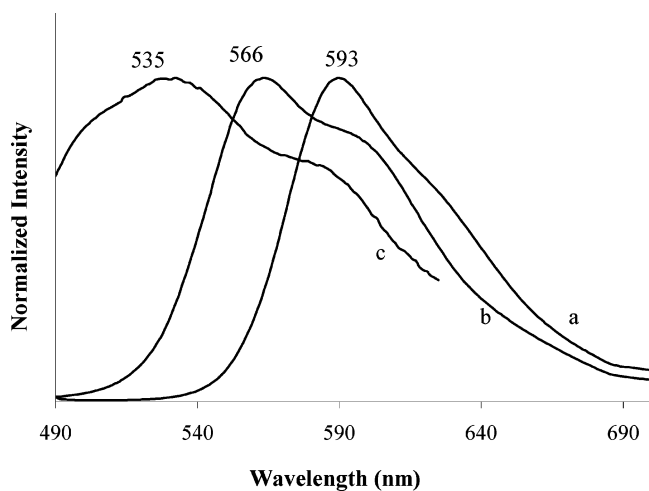


Figure 10. Emission spectra of (a) MEH-PPV, (b) the MEH-PPV/SBA-15 composite, and (c) the MEH-PPV/(SBA-15 with phenyltrimethoxysilane) composite.

Although the emission in solution is solvent dependent, the polymer in solution is less aggregated and has predominant intrachain excitations, which produce an emission at higher

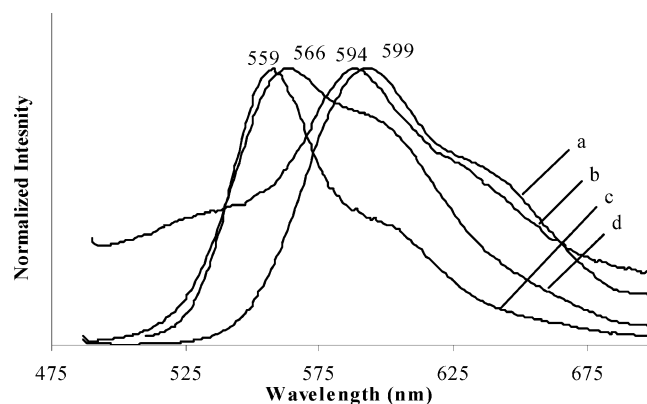


Figure 11. Comparative emission spectra of (a) MEH-PPV film, (b) MEH-PPV fibers, (c) MEH-PPV solution (10^{-7} M solution in 1,2-dichloroethane), and (d) MEH-PPV/SBA-15 composite fibers.

energy compared to that in the film. In the film where the polymer chains are more rigid, interchain excitations are also possible which lead to an emission at lower energy when compared to the solution. Similar red shifts in emission for solid-state samples of PPV oligomers when compared to solutions in CH_2Cl_2 was reported by Tian et al.²⁷ These shifts were attributed

to the increase in the HOMO–LUMO energy gap caused by conformational distortions in solutions. When the emission spectra of solution, film, and fibers of MEH-PPV were compared (spectra a and b in Figure 11), it was found that there was a blue shift in the emission for the fibers when compared to the film and a red shift when compared to solution (spectrum c in Figure 11). This suggests that, in the form of electrospun fibers, the polymer chains are not as rigid as in a film which might have caused a slight blue shift in the MEH-PPV fibers when compared to a film. A similar red shift in the emission of the fluorescent polymer poly[*p*-(phenylene ethynylene)alt(thienylene ethynylene)] (PPETE) fibers blended with poly(ethylene oxide) (PEO) was reported when compared to the solution.³²

When the emission spectra of MEH-PPV solution, film, and fibers and MEH-PPV/SBA-15 composite fibers are compared (Figure 11), the emission maximum of the composite (spectrum d in Figure 11) is red shifted compared to solution (10^{-7} molar) and blue shifted compared to pure MEH-PPV fibers and the film. This suggests that, in the composite, when compared to film there might be a prevention of aggregation, which might prevent π – π stacking between the phenyl rings to some extent electrospun in the fibers in general and even more so in the composite mesh. By a decrease in the π – π stacking, interchain electron delocalization can be decreased thereby shifting the emission to higher energies. However, even in the composite, the polymer chains may not be as spacially separated as in a solution which leads to a red shift compared to solution. It has been shown that the *cis*-conformer is more prone to interchain interactions at lower concentrations.⁸ Therefore, the presence of a predominantly *trans* configuration as suggested by the FTIR spectra may be a contributing factor in the observed emission shifts.

To further study the effect of aggregation, the absorption and emission spectra were recorded for various concentrations of MEH-PPV solution in 1,2-dichloroethane. As the concentration was decreased from 10^{-5} mol to 10^{-7} mol in the solution, there was a slight blue shift in absorption maximum from 512 to 509 nm with an increase in intensity.²⁴ Further dilution to 10^{-8} mol resulted in a broad peak with a λ_{max} of ~ 503 nm and decreased intensity. The emission spectra also showed a similar decrease in intensities and blue shifts in emission λ_{max} with a decrease in concentration.²⁴ As the concentration is decreased, interchain interactions decrease leading to a blue shift in absorption and emission. Up to a certain concentration, the intensity increases due to this phenomenon (comparing spectra of solutions with concentrations 10^{-5} and 10^{-7} mol). For very dilute solutions, the intensity decreases because of the lack of enough material to absorb or emit (10^{-8} molar solutions in the present case).

To further study the cause of the observed changes in fluorescence, the microphotoluminescence (microPL) spectra were recorded for a film, pure MEH-PPV fibers and MEH-PPV/SBA-15 composite fibers by exciting the samples with a 404 nm laser. These spectra were recorded by focusing onto broad leafy regions or fibrous regions of the fiber samples separately which produced an emission λ_{max} of 610 nm. The emission spectra obtained for the leafy region and a fibrous portion of the sample show emission λ_{max} values of 599 and 594 nm (broad peak), respectively. The blue shift in the case

of fiber samples compared to film is probably due to decreased interchain interactions in the polymer in the form of fibers as explained above. In addition, the higher surface of the fibers compared to a film, might probably prevent quenching from the surface. Also, the macroemission spectrum of the film (λ_{max} of 599 nm) corresponds to the emission λ_{max} of the leafy regions. The macroemission spectrum of the fibers (λ_{max} of 594 nm) probably reflects the overall effects of different regions in the fiber sample.

Figure 12a and b show the micro-PL spectra obtained for leafy and fibrous regions of the composite fiber samples along with the digital images of the sample regions focused. These two spectra show a λ_{max} value of 564 nm which corresponds well with the macroemission spectrum of the composite fibers (λ_{max} of 566 nm). The similarity in these spectra suggests that the polymer is essentially in the same state in both the regions. The blue shift in the micro-PL spectra of the composite fibers compared to pure MEH-PPV fibers strongly suggests that aggregation in the polymer is prevented when electrospun along with the SBA-15 material. In the composite, by electrospinning two different materials together, the silica material may serve as a nanospacer preventing the aggregation. This also is supported by the fact that the SEM images show fewer leafy regions for the polymer in the composite samples. However, the interchain interactions may not be as small as those in a dilute solution because the micro-PL spectra are also red shifted compared to the emission spectra of solution. A red shift in the emission when compared to MEH-PPV solution was reported for an ensemble of fluorescence measured for single molecules by Hu et al., and this was attributed to the possible defects in the molecules.³³

To study the effect of the molecular sieve fibers in the composites, organosilanes were partly substituted in the place of TMOS. Tolbert et al. had observed a blue shift in the emission of MEH-PPV where the polymer was encapsulated in the pores of MCM-41 (also a mesoporous silica) functionalized with trimethylchlorosilane (TMCS) and phenyldimethylchlorosilane (PDMCS) by a postsynthetic grafting.^{5,10,34} In contrast, we observe that when 3% of the silica source was substituted with either TMCS or PDMCS, no shift in the emission of MEH-PPV in MEH-PPV/SBA-15 composite was observed. In addition, no shift in emission was observed when MEH-PPV was electrospun separately on top of SBA-15 fibers. Therefore, the simple contact with SBA-15 does not alter the polymer structure. Another example, a physical mixture of MEH-PPV solution and an SBA-15 gel also did not change the fluorescence of the polymer. So only the intimate contact achieved in the electrospun mesh alters the polymer structure in a reversible manner. When the electrospun MEH-PPV fibers in a composite mesh were dissolved and the photoluminescence was recorded, it was found that the emission spectrum returned to the original starting bulk material.

When 3% of the silica source was substituted by phenyl trimethoxysilane (PhTMS), the blue shift in the polymer emission suggests an even stronger interaction with the molecular sieve. The composite samples now emit green with an emission λ_{max} of 535 nm (Figure 10c), and the excitation spectra

(32) Zhang, Y.; Dong, H.; Norris, I. D.; MacDiarmid, A.; Jones, W. E., Jr. *Polym. Mater. Sci. Eng.* **2001**, *85*, 622.

(33) Hu, D.; Yu, J.; Barbara, P. F. *J. Am. Chem. Soc.* **1999**, *121*, 6936.

(34) Tolbert, S. H.; Wu, J.; Gross, A. F.; Nguyen, T. Q.; Schwartz, B. J. *Microporous Mesoporous Mater.* **2001**, *44–45*, 445.

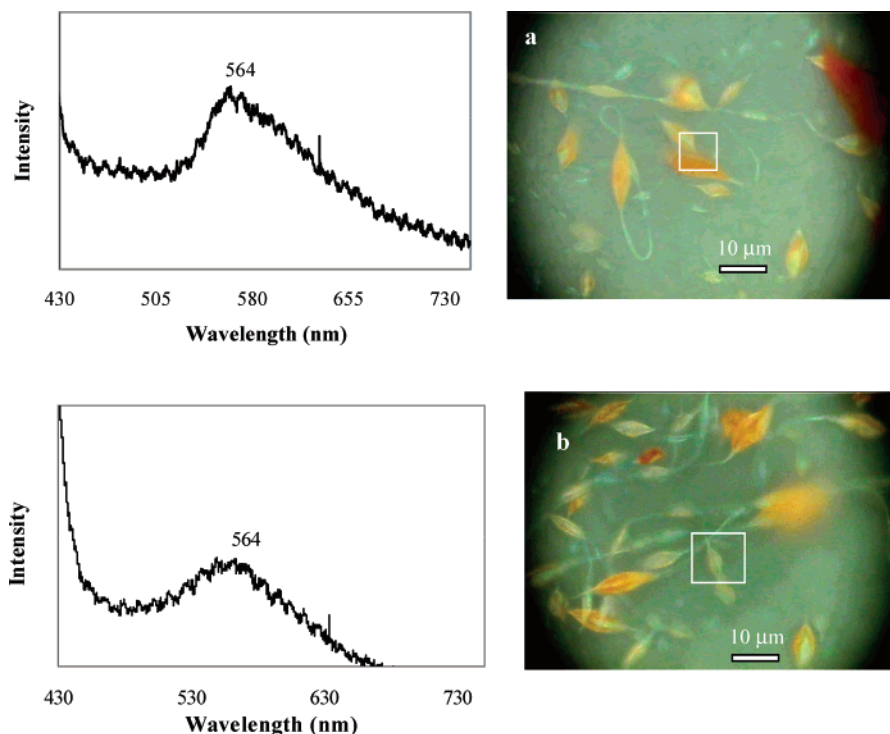


Figure 12. Microphotoluminescence spectra of MEH-PPV in MEH-PPV/SBA-15 electrospun composite fibers along with the digital images of the region focused on (a) a broad region of the fiber and (b) a thin fibrous region of the fiber.

show a new feature around 400 nm. To better explain the results, excitation spectra of the composite fibers were recorded with the emission wavelengths set at different values as before (Figure 5i (page S5) in the Supporting Information). Emission spectra were then recorded by exciting the sample at different regions in the electromagnetic spectrum (Figure 5ii (page S5) in the Supporting Information). When the excitation and emission spectra of MEH-PPV, MEH-PPV/SBA-15 composite, and MEH-PPV/(SBA-15 with phenyltrimethoxysilane) composite fibers are compared, it appears that there is no significant difference in excitation spectra. The new feature around 400 nm in the excitation spectrum is probably due to an underlying vibronic state which is being expressed by improving the order of the polymer chain. The absorption spectrum of highly oriented and structurally ordered MEH-PPV is shown to produce a series of vibrational sidebands.³⁵

Conclusion

In conclusion, we have shown that the electroluminescent polymer MEH-PPV can be electrospun into fibers, and the

optical properties can be altered by compositing it with an inorganic fiber material. The composites formed with SBA-15 show a blue shift in the emission, which can also be altered by introducing organic moieties into the inorganic material. The shift in the emission is mainly attributed to possible prevention of aggregation of the polymer chains, which might have been further influenced by the polymer chain conformation. The silica mesoporous fibers have acted as a nanospacer thereby reducing interchain interactions, resulting in the blue shift in the emission. In summary, dual syringe electrospinning may be a way to alter the optical properties of the fluorescent polymers in fibrous form, which may have interesting applications in the molecular electronics.

Acknowledgment. We thank the Robert A. Welch Foundation for Financial support of this research.

Supporting Information Available: Supporting Information includes a diagram of the electrospinning setup as well as excitation and emission spectra at various wavelengths for the polymer and composite fibers. This material is available free of charge via the Internet at <http://pubs.acs.org>.

(35) Hagler, T. W.; Pakbaz, K.; Voss, F.; Heeger, A. J. *Phys. Rev. B* **1991**, *44*, 8652.